STABILITY ANALYSIS OF TIME-PERIODIC SYSTEMS USING MULTIBODY SIMULATION FOR APPLICATION TO HELICOPTERS

A. Rezaeian, German Aerospace Center, Institute of Aeroelasticity,
Bunsenstraße 10, 37073 Göttingen, Germany
alireza.rezaeian@dlr.de

Abstract

Helicopters are rotating systems with time-periodic characteristics. It means some parameters of the system, e.g. aerodynamic forces, change periodically during the one revolution of a rotor blade. There are simulation tools like “CAMRAD II” for modelling and analysing of any type of rotor-craft like helicopters or tilt-rotors. However, these tools are often limited for a range of special tasks. The aim of this paper [1] is to investigate the multibody simulation tool “SIMPACK” for the stability analysis of a rotating system. Stability or instability is related to the behaviour of a system in the equilibrium state due to a small disturbance. Among all the existing methods of the stability analysis of a time-periodic system “Floquet theory” and “Multiblade coordinates transformation” are applied. Starting from a nonlinear system with time-periodic characteristics, the equilibrium state is first established. This equilibrium state can be static or dynamic (dynamic state: helicopter in forward flight). The system is then linearised about the equilibrium state. Using the Floquet theory allows to predict the stability or instability of the linearised time-periodic system without usage of any approximations. Using the multiblade coordinates transformation allows first reducing the number of periodic terms in the first order linear differential equations of motion of the system. A time average approximation of the remaining periodic terms changes the equations to the linear differential equations with constant coefficients. Afterward for the stability analysis of this approximated equation the classical stability analysis method “Eigenvalue Analysis” is used.

1. INTRODUCTION

Mathematical models of an aeromechanical system can be given in a form of differential equation or systems of differential equations. In general the differential equation of motion can be non-linear with time dependent coefficients. When the time dependent coefficients are time-periodic, the system is then called time-periodic system.

Often rotating systems, in which at least one part rotates, belong to this group. Helicopters are in fact rotating system with mostly non-linear dynamics. For helicopters the basic source of nonlinearities come from inertia, elastic and aerodynamic forces. Beyond these basic sources of nonlinearities other sources exist as well. For example hydraulic dampers and devices, which are characterized by velocity squared, cause the nonlinearities of the system. The investigation of the dynamics of a rotating system and its stability analysis is not something new. The first flowering of rotor dynamic literature happened in the decade following World War I [2]. Several instability mechanisms [3] for rotor whirl were identified by Prandtl. A graphical tool for predicting critical speeds was introduced by Cambell [4]. The second period of progress of rotor dynamics began in 1960s, with the introduction of improved instrumentation and data processing tools. Beginning in 1967 the ASME (**A**merican **S**ociety of **M**echanical **E**ngineering) has held vibration conferences every two years which increased the knowledge on rotor dynamics. There are many research groups, which work on the dynamic behaviour of rotating systems. It seems the rotor dynamics has separated itself from the subdiscipline of vibration.

Testing of the rotorcraft aeroelastic stability is a necessary step for the successful development of new designs. There are special tools which are able to simulate and predict the aeroelastic behaviour of a system, however the high level of accuracy for a complex aeroelastic problem is still challenging and in some cases experimental tests are inevitable. Testing a prototype at full scale or model scale is typically very expensive. Therefore more investigation on improvement and optimization of the computational methods and modelling tools is needed.

The aeroelastic instability happens less frequently but ends more dramatically. A vibratory mode of a rotor can be stable over a wide range of operating conditions and with a small change in speed or torque may become violently unstable with a rapid growth in amplitude leading either to failure or to a limit cycle if nonlinearities limit the growth. Aeroelastic instability limits the operational range. For helicopters the maximum speed is limited by the power available, stall, compressibility and aeroelastic stability effects. Having deep knowledge of the physics of an aeroelastic instability of a system allows finding solutions to prevent the instability. Parametric analysis using simulation tools enable us to investigate the effects of different system parameters on those limits.

The aeroelastic stability of the time-periodic systems can be evaluated by using a nonlinear analysis to calculate the transient response of the system. The disadvantages of this approach are that much more computation is needed to obtain the transient response than to obtain the periodic solution (which in fact must be obtained first as a starting point for the transient motion), and it is difficult to obtain quantitative information about the complete dynamics from the transient response. An alternative approach is to calculate aeroelastic stability using the

methods of linear system theory. Therefore linearization is a preliminary step to apply these linear methods.
It is assumed that, the nonlinear differential equation of a system can be given by:

(1) $\dot{x}_i = f_i(x_1, x_2, \ldots, x_n)$

Applying the Jacobian linearization method with consideration of the linearization point *"LP"* results the following linear equation:

(2) $$\dot{X} = \begin{bmatrix} \dot{X}_1 \\ \dot{X}_2 \\ \vdots \\ \dot{X}_n \end{bmatrix} = \begin{bmatrix} \left.\frac{\partial f_1}{\partial x_1}\right|_{LP} & \left.\frac{\partial f_1}{\partial x_2}\right|_{LP} & \cdots & \left.\frac{\partial f_1}{\partial x_n}\right|_{LP} \\ \left.\frac{\partial f_2}{\partial x_1}\right|_{LP} & \left.\frac{\partial f_2}{\partial x_2}\right|_{LP} & \cdots & \left.\frac{\partial f_2}{\partial x_n}\right|_{LP} \\ \vdots & \vdots & \vdots & \vdots \\ \left.\frac{\partial f_n}{\partial x_1}\right|_{LP} & \left.\frac{\partial f_n}{\partial x_2}\right|_{LP} & \cdots & \left.\frac{\partial f_n}{\partial x_n}\right|_{LP} \end{bmatrix} \cdot \begin{bmatrix} X_1 \\ X_2 \\ \vdots \\ X_n \end{bmatrix}$$

This equation can be rewritten in the following form:

(3) $\dot{X} = [A] \cdot X$

The matrix $[A]$ is called "system matrix".

For the stability analysis of the linear equation (3) following methods can be performed:

- If the system matrix is constant in time, then eigenvalue analysis will be the solution.
- If the system matrix is time dependent and periodic the first method is to use the Floquet theory, which gives the exact solution.
  the second method is to use an approximation method to change the system matrix to a constant matrix and then performing the eigenvalue analysis.

1.1. Stability analysis based on Floquet theory

Floquet Theory is one of the widely used methods for predicting the stability of a system with periodic coefficients from knowledge of the eigenvalues of the Floquet transient matrix. In classical application of Floquet theory, this matrix is explicitly evaluated and then its eigenvalues are computed. The implicit Floquet analysis is another method that extracts the dominant eignevalues of the Floquet transient matrix without the explicit computation of this matrix. This method relies on the properties of the Arnoldi algorithm (one of the most reliable methods for extracting the eigenvalues of a general matrix of size NxN) [5].
Floquet analysis of rotorcraft began with Ref [6] which utilized a "rectangular ripple" method to generate the transition matrix [7]. The introduction of conventional time-marching Floquet analysis began with Ref [8]. The most significant improvement in computational efficiency came from the so called "single pass method" [9, 10]. The accuracy of the Floquet transition matrix depends only upon the computational procedures used. If the accuracies of the Floquet transition matrix and the eigenvalue routine are known, then the bounds of accuracy on the stability boundaries can be determined.
Consider a system with n states. For this system n solutions for one period at the end of n possible linearly independent initial conditions should be created. These solutions build the transition matrix at $t = T$ (end of one period). After creating this matrix, one must find the eigenvalues of the transition matrix. To find the frequency and damping of each mode, one must take the logarithm of the calculated eigenvalues.

Considering the following linear periodic equation

(4) $\dot{Z} = [A(t+T)] \cdot Z$

Floquet's Theorem states that an *nth* order system of ordinary differential equations, having periodic coefficients, has transient solution of the form:

(5) $Z(t) = \Phi(t) \cdot \Phi^{-1}(0) \cdot Z(0) = \Phi(t,0) \cdot Z(0)$

With the definition of a new function $Q(t)$

(6) $Q(t) = \Phi(t,0) \cdot e^{-Bt}$

$\Phi(t,0) \equiv$ fundamental matrix

the transient solution (5) can be written in the form:

(7) $Z(t) = Q(t) \cdot e^{Bt}.Z(0)$

It can be proved that $Q(t)$ is a periodic function ($Q(t+T) = Q(t)$) and $Z(0) = constant$, therefore the stability or instability of the solution (7) depends on "e^{Bt}" or "B". The fundamental matrix is regular therefore it can be proved that:

(8) $[\Phi(T,0)] = [\Phi_1 \quad \cdots \quad \Phi_n] = e^{BT}$

Equation (9) is used to calculate the columns of the fundamental matrix given by (8).

(9) $[Z(T)] = [\Phi(T,0)] \cdot [Z(0)]$

Consider a system with n states (fundamental matrix with n columns). For this system n solutions for one period at the end of n possible linearly independent initial conditions should be calculated. These solutions build the transition matrix at $t = T$ (end of one period).

(10) $$\begin{bmatrix} Z_1(0) \\ \vdots \\ \dot{Z}_{n/2}(0) \end{bmatrix} = \begin{bmatrix} 1 \\ \vdots \\ 0 \end{bmatrix} \xrightarrow{\int_0^T linear-system} \begin{bmatrix} Z_1(T) \\ \vdots \\ \dot{Z}_{n/2}(T) \end{bmatrix} = [\Phi_1] = \begin{bmatrix} \phi_{11} \\ \vdots \\ \varphi_{1n} \end{bmatrix}$$
$$\vdots$$
$$\begin{bmatrix} Z_1(0) \\ \vdots \\ \dot{Z}_{n/2}(0) \end{bmatrix} = \begin{bmatrix} 0 \\ \vdots \\ 1 \end{bmatrix} \xrightarrow{\int_0^T linear-system} \begin{bmatrix} Z_1(T) \\ \vdots \\ \dot{Z}_{n/2}(T) \end{bmatrix} = [\Phi_n] = \begin{bmatrix} \phi_{n1} \\ \vdots \\ \varphi_{nn} \end{bmatrix}$$

After creating the fundamental matrix, one should find the eigenvalues of the transition matrix. These eigenvalues are called "characteristic multipliers":

(11) $\lambda_j = \alpha_j \pm i\beta_j$

To find the frequency and damping of each mode the logarithm of the calculated characteristic multipliers should be calculated. Inserting the characteristic multipliers in the equation (12) allows calculating the characteristic exponents which are in fact the eigenvalues of matrix B .

(12) $\mu_j = \frac{1}{2T}\ln\left(\alpha_j^{\,2} + \beta_j^{\,2}\right) + i\frac{1}{T}\arctan\frac{\beta_j}{\alpha_j} = \mu_{j,R} + i\mu_{j,I}$

After calculation of the characteristic exponents if

$\mu_{j,R} \prec 0 \Rightarrow$ **asymptotic stable**

$\mu_{j,R} = 0 \Rightarrow$ **stability bound**

$\mu_{j,R} \succ 0 \Rightarrow$ **unstable**

1.2. Multiblade Coordinates

Generally the equation of motion of the rotor is derived in the rotating frame. In this frame each rotor blade is considered separately but mostly the rotor responds as a whole to an excitation. Changing the coordinate system from rotating to the nonrotating allows to analyse the rotor as a whole system. In the nonrotating frame the so called "multiblade coordinates" are defined. Transforming the differential equations of the motion from rotating frame to nonrotating frame has the following advantages:

- It simplifies the analysis and helps to understand the behaviour of the rotating system, especially, when they are in interaction with nonrotating parts.
- In the case of time-periodic system, the transformation reduces the number of time-periodic elements in the differential equations.
- A combination of multiblade transformation and time average approximation leads to a system of differential equation with constant coefficients.

Consider a rotor with N equally spaced blades. The azimuth of the i*th* blade is given by:

(13) $\psi_i = \psi_1 + (N-1)\frac{2\pi}{N}$

ψ_1 is the azimuth of the first blade. The arbitrary degree of freedom of the rotor blade " β "is then expressed in the multiblade coordinates as follows:

(14) $\beta_i = \beta_0 + \sum_{1}^{n}(\beta_{nc}\cos n\psi_i + \beta_{ns}\sin n\psi_i) + \beta_d(-1)^i$

with $n = 1$ to $\frac{N-2}{2}$ when N even

or $n = 1$ to $\frac{N-1}{2}$ when N odd

β_d appears only when N is even.

The multiblade coordinates from (14) are then calculated by following equations:

(15) $\beta_0 = \frac{1}{N}\sum_{i=1}^{N}(\beta_i)$ collective coordinate

(16) $\beta_d = \frac{1}{N}\sum_{i=1}^{N}\left(\beta_i \cdot (-1)^i\right)$ differential coordinate

(17) $\beta_{nc} = \frac{2}{N}\sum_{i=1}^{N}(\beta_i \cos n\psi_i)$ cyclic coordinate

(18) $\beta_{ns} = \frac{2}{N}\sum_{i=1}^{N}(\beta_i \sin n\psi_i)$ cyclic coordinate

These coordinates defines the new degrees of freedom, which describe the motion of the rotor as a whole in a fixed frame. Fig. 1 shows as an example the multiblade modes of flapping motion of a four bladed rotor in nonrotating frame

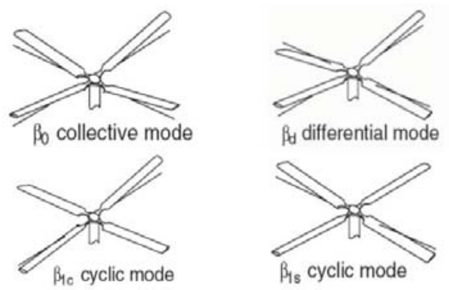

FIG. 1. Multiblade modes of flapping rotor blade

There are similarities between the multiblade coordinates and Fourier series but they are not the same. If the motion in the rotating frame represented by a Fourier series, then the coefficients of series are constant in time but infinite in number. Multiblade coordinates transformation allows to integrate the dynamics of individual blades and express them in a nonrotating frame. Normally this transformation has two steps:

- Transformation of the rotating degree of freedom
- Transformation of the equation of motion

multiblade transformation is used widely in the helicopter branch. The first successful try to understand the ground resonance problem was done with help of multiblade coordinates [11]. Johnson [12] provided a mathematical basis for multiblade coordinates. Using this helps to develop a numerical coordinate transformation, this can be used for stability analysis of a rotating system modelled with a simulation tool.

1.3. Simulation tool SIMPACK

SIMPACK (**SI**mulation of **M**ulti-body systems **PACK**age) software package is used to simulate, analyse and design all types of mechanical system. It can analyse the vibrational behaviour of multi-body systems and allows predicting and describing the motion of a complex machine or mechanisms. The software was developed at the German Aerospace Research Centre (DLR) together with INTEC GmbH, with important practical enhancements added to the software at MAN Technology AG [13].The software has a comprehensive range of modelling and calculation features. Therefore it is applied within industry, university and research institutions. There are different modelling elements, which are used to simulate a complex system. Data related to these elements can be entered in to SIMPACK via the graphical user interface. Most important modelling elements are:

- Reference Frames
- Bodies
- Joints, Constraints
- Force elements
- Sensors, Control elements
- Substructures, Substitutions variables

SIMPACK creates first of all the equations of motion for a modelled mechanical system and then solves it with different mathematical procedures. A wide range of analyses features are available to analyse dynamic systems. These are:

- Static Analysis
- Kinematics Analysis
- Non-linear Dynamic Analysis
- Linear System Analysis
- Symbolic Code Generation
- Eigenvalue Analysis

2. APPLICATION OF FLOQUET THEORY USING SIMPACK

For the stability analysis of a time-periodic system modelled using SIMPACK following procedures are performed:

1) Finding the equilibrium state, founded equilibrium state is saved as linearization state
2) Defining the state variables of the system
3) Defining the period T of the time-periodic system
4) For a system with *n* state variables, *n* independent initial states are defined. The best way to make *n* independent initial states is for each initial state one state parameter is non zero and all other will be zero.
5) For each initial state the "linear time integration" option of SIMPACK is used to integrate the system from initial state to the end of one period.
6) The values of the state variables at the end of the integration are then saved. Each integration produces one column of the fundamental matrix
7) Determining the fundamental matrix
8) Calculation of eigenvalues (characteristic multipliers) of the fundamental matrix
9) Calculation of characteristic exponents
10) Interpretation of the results

2.1. Example periodic mass-spring-damper

To evealuate the stability analysis procedures mentioned above a mass-spring-damper system with periodic coefficients is modelled using SIMPACK. Fig. 2 shows this model. The idea of this example comes from paper [14].

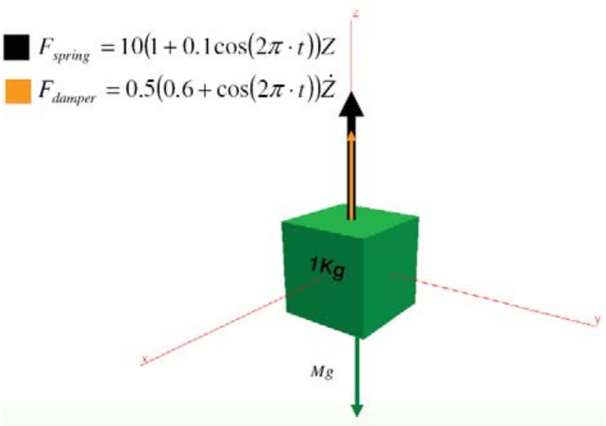

FIG. 2. SIMPACK mass-spring-damper model

The motion of this system is defined with the linear differential equation (19).

$$(19) \quad \ddot{Z} + 0.4(0.5 + \cos(2\pi \cdot t))\dot{Z} + 10(1 + 0.1\cos(2\pi \cdot t))Z = 0$$

Considering the state variables Z and $\dot{Z}$, equation (19) can be written in the new form of the system of first order differential equations given by equation (20).

$$(20) \quad \begin{bmatrix} \dot{Z} \\ \ddot{Z} \end{bmatrix} = \begin{bmatrix} 0 & 1 \\ -10(1+0.1\cos(2\pi \cdot t)) & -0.5(0.6+\cos(2\pi \cdot t)) \end{bmatrix} \cdot \begin{bmatrix} Z \\ \dot{Z} \end{bmatrix}$$

Now two independent initial states are defined and then the system is integrated. Equations (21) and (22) show these procedures.

$$(21) \quad \begin{bmatrix} Z(0) \\ \dot{Z}(0) \end{bmatrix} = \begin{bmatrix} 0.1 \\ 0 \end{bmatrix} \xrightarrow{\int_0^T SIMPACK} \begin{bmatrix} Z(T) \\ \dot{Z}(T) \end{bmatrix} = \begin{bmatrix} -0.0977 \\ 0.02845 \end{bmatrix} = \begin{bmatrix} \phi_{11} & \phi_{12} \\ \phi_{21} & \phi_{22} \end{bmatrix} \cdot \begin{bmatrix} 0.1 \\ 0 \end{bmatrix}$$

$$(22) \quad \begin{bmatrix} Z(0) \\ \dot{Z}(0) \end{bmatrix} = \begin{bmatrix} 0 \\ 0.1 \end{bmatrix} \xrightarrow{\int_0^T SIMPACK} \begin{bmatrix} Z(T) \\ \dot{Z}(T) \end{bmatrix} = \begin{bmatrix} 0.00150 \\ -0.07656 \end{bmatrix} = \begin{bmatrix} \phi_{11} & \phi_{12} \\ \phi_{21} & \phi_{22} \end{bmatrix} \cdot \begin{bmatrix} 0 \\ 0.1 \end{bmatrix}$$

Using the equations (21) and (22) the elements of the fundamental matrix (23) are calculated.

$$(23) \quad [\Phi(T,0)] = \begin{bmatrix} \phi_{11} & \phi_{12} \\ \phi_{21} & \phi_{22} \end{bmatrix} = \begin{bmatrix} -0.9770 & 0.0150 \\ 0.2845 & -0.7655 \end{bmatrix}$$

Calculating the characteristic exponent shows the stability of the system.

$\mu_{1,R} = -0.004 \prec 0$ stable system

$\mu_{2,R} = -0.29 \prec 0$ stable system

The direct time integration of the system (equation (19)) using SIMPACK shows the stability of the system. The state variables after a small disturbance converge to initial state (linearization state). Calculating the eigenvalues of the system matrix, given by equation (20), shows that, the real part of the eigenvalues in one period of oscillation changes from a positive value to a negative one which results positive and negative damping of the system in one period. According to the classical stability analysis it is not clear whether this system is stable or not.

3. APPLICATION OF MULTIBLADE COORDINATES TRANSFORMATION USING SIMPACK

For stability analysis using multiblade coordinate transformation for SIMPACK model the following steps are performed:

1) Finding the equilibrium state
2) Linearising the system about the equilibrium state. In the case of dynamic equilibrium state (for helicopter rotor in forward flight), one period of dynamic equilibrium state is divided to finite number of time steps. For each time step of one period the values of state variables are saved and then the system is linearised about this point.
3) Calculation of the system matrix from the linearised system. SIMPACK allows producing the system matrices in MATLAB m-file format.

4) Multiblade coordinates transformation of the linear system matrix. This transformation is done using implemented MATLAB program.
5) For a system with dynamic equilibrium state, step 3 and 4 are repeated for the all time steps of one period.
6) Constant coefficient approximation .Constant coefficient approximation is then made by calculating the time average of the multiblade transformed system matrices.
7) Performing the eigenvalue analysis for the time averaged transformed system matrix resulted from step 6.
8) Repeating the steps 1 to 7 for different system parameters. For example different rotor rotational velocity.
9) Post-processing of the results. This can be done for example with post-processing option of SIMPACK, MATLAB or with EXCEL.

To implement the multiblade coordinates transformation in MATLAB program, first of all this transformation should be mathematically formulated. For transformation two different methods have been established. Implementing the both methods has the advantage of validation of the transformation formulations. The both methods should result the same values.

3.1. First mathematical method of multiblade coordinates transformation

For describing the transformation methods, to avoid the complexity, an isolated four bladed rotor is considered. To each blade belongs stiffness and damping and blades are uncoupled. Equation (24) gives the linear differential equation of this isolated rotor. β is an arbitrary degree of freedom.

(24) $$\begin{bmatrix}\dot\beta_1\\\dot\beta_2\\\dot\beta_3\\\dot\beta_4\\\ddot\beta_1\\\ddot\beta_2\\\ddot\beta_3\\\ddot\beta_4\end{bmatrix}=\begin{bmatrix}0&0&0&0&1&0&0&0\\0&0&0&0&0&1&0&0\\0&0&0&0&0&0&1&0\\0&0&0&0&0&0&0&1\\a_{51}&0&0&0&a_{55}&0&0&0\\0&a_{62}&0&0&0&a_{66}&0&0\\0&0&a_{73}&0&0&0&a_{77}&0\\0&0&0&a_{84}&0&0&0&a_{88}\end{bmatrix}\cdot\begin{bmatrix}\beta_1\\\beta_2\\\beta_3\\\beta_4\\\dot\beta_1\\\dot\beta_2\\\dot\beta_3\\\dot\beta_4\end{bmatrix}$$

According to equation (24) one can write:

(25) $\ddot\beta_1 = a_{51}\cdot\beta_1 + a_{55}\cdot\dot\beta_1$

For a four bladed rotor equation (26) and (27) gives the degree of freedom "β" and respectively "$\dot\beta$" in multiblade coordinates.

(26) $$\beta_i = \beta_0 + \beta_{1c}\cdot\cos\left(\psi+\frac{(i-1)}{2}\pi\right) + \beta_{1s}\cdot\sin\left(\psi+\frac{(i-1)}{2}\pi\right) + \beta_d = \begin{bmatrix}1 & \cos\left(\psi+\frac{(i-1)}{2}\pi\right) & \sin\left(\psi+\frac{(i-1)}{2}\pi\right) & (-1)^i\end{bmatrix}\cdot\begin{bmatrix}\beta_0\\\beta_{1c}\\\beta_{1s}\\\beta_d\end{bmatrix}$$

(27) $$\dot\beta_i = \begin{bmatrix}0 & -\Omega\sin\left(\psi+\frac{(i-1)}{2}\pi\right) & \Omega\cos\left(\psi+\frac{(i-1)}{2}\pi\right) & 0\end{bmatrix}\cdot\begin{bmatrix}\beta_0\\\beta_{1c}\\\beta_{1s}\\\beta_d\end{bmatrix} + \begin{bmatrix}1 & \cos\left(\psi+\frac{(i-1)}{2}\pi\right) & \sin\left(\psi+\frac{(i-1)}{2}\pi\right) & (-1)^i\end{bmatrix}\cdot\begin{bmatrix}\dot\beta_0\\\dot\beta_{1c}\\\dot\beta_{1s}\\\dot\theta_d\end{bmatrix}$$

Substituting equation (26) and (27) in equation (25) and rewriting it for all rotor blades results in equation (28).

(28) $$\begin{bmatrix}\ddot\beta_1\\\ddot\beta_2\\\ddot\beta_3\\\ddot\beta_4\end{bmatrix}=\begin{bmatrix}a_{51} & a_{51}\cos(\psi) & a_{51}\sin(\psi) & -a_{51}\\ a_{62} & a_{62}\cos\left(\psi+\frac{\pi}{2}\right) & a_{62}\sin\left(\psi+\frac{\pi}{2}\right) & a_{62}\\ a_{73} & a_{73}\cos(\psi+\pi) & a_{73}\sin(\psi+\pi) & -a_{73}\\ a_{84} & a_{84}\cos\left(\psi+\frac{3\pi}{2}\right) & a_{84}\sin\left(\psi+\frac{3\pi}{2}\right) & a_{84}\end{bmatrix}\cdot\begin{bmatrix}\beta_0\\\beta_{1c}\\\beta_{1s}\\\beta_d\end{bmatrix}+$$
$$\begin{bmatrix}0 & -a_{55}\Omega\sin(\psi) & a_{55}\Omega\cos(\psi) & 0\\ 0 & -a_{66}\Omega\sin\left(\psi+\frac{\pi}{2}\right) & a_{66}\Omega\cos\left(\psi+\frac{\pi}{2}\right) & 0\\ 0 & -a_{77}\Omega\sin(\psi+\pi) & a_{77}\Omega\cos(\psi+\pi) & 0\\ 0 & -a_{88}\Omega\sin\left(\psi+\frac{3\pi}{2}\right) & a_{88}\Omega\cos\left(\psi+\frac{3\pi}{2}\right) & 0\end{bmatrix}\cdot\begin{bmatrix}\beta_0\\\beta_{1c}\\\beta_{1s}\\\beta_d\end{bmatrix}$$
$$\begin{bmatrix}a_{55} & a_{55}\cos(\psi) & a_{55}\sin(\psi) & -a_{55}\\ a_{66} & a_{66}\cos\left(\psi+\frac{\pi}{2}\right) & a_{66}\sin\left(\psi+\frac{\pi}{2}\right) & a_{66}\\ a_{77} & a_{77}\cos(\psi+\pi) & a_{77}\sin(\psi+\pi) & -a_{77}\\ a_{88} & a_{88}\cos\left(\psi+\frac{3\pi}{2}\right) & a_{88}\sin\left(\psi+\frac{3\pi}{2}\right) & a_{88}\end{bmatrix}\cdot\begin{bmatrix}\dot\beta_0\\\dot\beta_{1c}\\\dot\beta_{1s}\\\dot\beta_d\end{bmatrix}$$

On the other hand, the second derivative of β in multiblade coordinates is given by:

(29) $$\ddot\beta_i = \begin{bmatrix}0 & -\Omega^2\cos\left(\psi+\frac{(i-1)}{2}\pi\right) & -\Omega^2\sin\left(\psi+\frac{(i-1)}{2}\pi\right) & 0\end{bmatrix}\cdot\begin{bmatrix}\beta_0\\\beta_{1c}\\\beta_{1s}\\\beta_d\end{bmatrix}+$$
$$\begin{bmatrix}0 & -2\Omega\sin\left(\psi+\frac{(i-1)}{2}\pi\right) & 2\Omega\cos\left(\psi+\frac{(i-1)}{2}\pi\right) & 0\end{bmatrix}\cdot\begin{bmatrix}\dot\beta_0\\\dot\beta_{1c}\\\dot\beta_{1s}\\\dot\beta_d\end{bmatrix}+$$
$$\begin{bmatrix}1 & \cos\left(\psi+\frac{(i-1)}{2}\pi\right) & \sin\left(\psi+\frac{(i-1)}{2}\pi\right) & (-1)^i\end{bmatrix}\cdot\begin{bmatrix}\ddot\beta_0\\\ddot\beta_{1c}\\\ddot\beta_{1s}\\\ddot\beta_d\end{bmatrix}$$

Writing equation (29) for all the four blades results:

$$\begin{bmatrix}\ddot\beta_1\\\ddot\beta_2\\\ddot\beta_3\\\ddot\beta_4\end{bmatrix}=\begin{bmatrix}0 & -\Omega^2\cos(\psi) & -\Omega^2\sin(\psi) & 0\\0 & -\Omega^2\cos\left(\psi+\frac{\pi}{2}\right) & -\Omega^2\sin\left(\psi+\frac{\pi}{2}\right) & 0\\0 & -\Omega^2\cos(\psi+\pi) & -\Omega^2\sin(\psi+\pi) & 0\\0 & -\Omega^2\cos\left(\psi+\frac{3\pi}{2}\right) & -\Omega^2\sin\left(\psi+\frac{3\pi}{2}\right) & 0\end{bmatrix}\cdot\begin{bmatrix}\beta_0\\\beta_{1c}\\\beta_{1s}\\\beta_d\end{bmatrix}+$$

$$\begin{bmatrix}0 & -2\Omega\sin(\psi) & 2\Omega\cos(\psi) & 0\\0 & -2\Omega\sin\left(\psi+\frac{\pi}{2}\right) & 2\Omega\cos\left(\psi+\frac{\pi}{2}\right) & 0\\0 & -2\Omega\sin(\psi+\pi) & 2\Omega\cos(\psi+\pi) & 0\\0 & -2\Omega\sin\left(\psi+\frac{3\pi}{2}\right) & 2\Omega\cos\left(\psi+\frac{3\pi}{2}\right) & 0\end{bmatrix}\cdot\begin{bmatrix}\dot\beta_0\\\dot\beta_{1c}\\\dot\beta_{1s}\\\dot\beta_d\end{bmatrix}+ \quad (30)$$

$$\begin{bmatrix}1 & \cos(\psi) & \sin(\psi) & -1\\1 & \cos\left(\psi+\frac{\pi}{2}\right) & \sin\left(\psi+\frac{\pi}{2}\right) & 1\\1 & \cos(\psi+\pi) & \sin(\psi+\pi) & -1\\1 & \cos\left(\psi+\frac{3\pi}{2}\right) & \sin\left(\psi+\frac{3\pi}{2}\right) & 1\end{bmatrix}\cdot\begin{bmatrix}\ddot\beta_0\\\ddot\beta_{1c}\\\ddot\beta_{1s}\\\ddot\beta_d\end{bmatrix}$$

Comparison of equations (28) and (30) led to a new equation. This equation gives the second derivative of multiblade coordinates as a function of multiblade coordinates and their first derivatives. This allows writing the final transformation result in the form given by equation (31). The elements of Matrices $[M]$ and $[N]$ are function of the elements of the linearised system matrix (24), azimuth and rotor rotational velocity.

$$\begin{bmatrix}\dot\beta_0\\\dot\beta_{1c}\\\dot\beta_{1s}\\\dot\beta_d\\\ddot\beta_0\\\ddot\beta_{1c}\\\ddot\beta_{1s}\\\ddot\beta_d\end{bmatrix}=\begin{bmatrix}[0] & [I]\\ [L]^{-1}\cdot[M] & [L]^{-1}\cdot[N]\end{bmatrix}\cdot\begin{bmatrix}\beta_0\\\beta_{1c}\\\beta_{1s}\\\beta_d\\\dot\beta_0\\\dot\beta_{1c}\\\dot\beta_{1s}\\\dot\beta_d\end{bmatrix} \quad (31)$$

The matrix $[L]$ is given by equation (32).

$$[L]=\begin{bmatrix}1 & \cos(\psi) & \sin(\psi) & -1\\1 & \cos\left(\psi+\frac{\pi}{2}\right) & \sin\left(\psi+\frac{\pi}{2}\right) & 1\\1 & \cos(\psi+\pi) & \sin(\psi+\pi) & -1\\1 & \cos\left(\psi+\frac{3\pi}{2}\right) & \sin\left(\psi+\frac{3\pi}{2}\right) & 1\end{bmatrix} \quad (32)$$

This method is used to transform a general system matrix, by which most elements due to the couple effects are nonzero [1].

3.2. Second mathematical method of multiblade coordinates transformation

For describing the second method of transformation, again the linear equation of motion of an isolated rotor given by equation (24) is considered. Equation (33) is obtained from equation (24).

$$\ddot\beta_1+\ddot\beta_2+\ddot\beta_3+\ddot\beta_4=a_{51}\beta_1+a_{55}\dot\beta_1+a_{62}\beta_2+a_{77}\dot\beta_2+a_{73}\beta_3+a_{77}\dot\beta_3+a_{84}\beta_4+a_{88}\dot\beta_4 \quad (33)$$

Writing the equation (29) for four blades and adding them together results:

$$\ddot\beta_1+\ddot\beta_2+\ddot\beta_3+\ddot\beta_4=\begin{bmatrix}4 & 0 & 0 & 0\end{bmatrix}\cdot\begin{bmatrix}\ddot\beta_0\\\ddot\beta_{1c}\\\ddot\beta_{1s}\\\ddot\beta_d\end{bmatrix} \quad (34)$$

Substitution of multiblade coordinates for the degree of freedom β and its derivative on the right side of equation (33) and making it equal to the right side of equation (34) allows determining elements $T_{5,i}$ of the transformed matrix given by equation (35).

$$\begin{bmatrix}\dot\beta_0\\\dot\beta_{1c}\\\dot\beta_{1s}\\\dot\beta_d\\\ddot\beta_0\\\ddot\beta_{1c}\\\ddot\beta_{1s}\\\ddot\beta_d\end{bmatrix}=\begin{bmatrix}0&0&0&0&1&0&0&0\\0&0&0&0&0&1&0&0\\0&0&0&0&0&0&1&0\\0&0&0&0&0&0&0&1\\T_{51}&T_{52}&T_{53}&T_{54}&T_{55}&T_{56}&T_{57}&T_{58}\\T_{61}&T_{62}&T_{63}&T_{64}&T_{65}&T_{66}&T_{67}&T_{68}\\T_{71}&T_{72}&T_{73}&T_{74}&T_{75}&T_{76}&T_{77}&T_{78}\\T_{81}&T_{82}&T_{83}&T_{84}&T_{85}&T_{86}&T_{87}&T_{88}\end{bmatrix}\cdot\begin{bmatrix}\beta_0\\\beta_{1c}\\\beta_{1s}\\\beta_d\\\dot\beta_0\\\dot\beta_{1c}\\\dot\beta_{1s}\\\dot\beta_d\end{bmatrix} \quad (35)$$

As an example, element $T_{5,1}$ is calculated as given by (36):

$$T_{51}=\frac{a_{51}+a_{62}+a_{73}+a_{84}}{4} \quad (36)$$

To calculate the element $T_{6,i}$ of the transformed matrix first the equation (29) is multiplied with:

$$\cos\left(\psi+\frac{(i-1)\pi}{2}\right)$$

Then for four blades the results of multiplication are added together as shown by equation (37).

$$\ddot\beta_1\cos(\psi)+\ddot\beta_2\cos\left(\psi+\frac{\pi}{2}\right)+\ddot\beta_3\cos(\psi+\pi)+\ddot\beta_4\cos\left(\psi+\frac{3\pi}{2}\right)=$$

$$\begin{bmatrix}0&2&0&0\end{bmatrix}\cdot\begin{bmatrix}\ddot\beta_0\\\ddot\beta_{1c}\\\ddot\beta_{1s}\\\ddot\beta_d\end{bmatrix}+\begin{bmatrix}0&0&4\Omega&0\end{bmatrix}\cdot\begin{bmatrix}\dot\beta_0\\\dot\beta_{1c}\\\dot\beta_{1s}\\\dot\beta_d\end{bmatrix}+ \quad (37)$$

$$\begin{bmatrix}0&-2\Omega^2&0&0\end{bmatrix}\cdot\begin{bmatrix}\beta_0\\\beta_{1c}\\\beta_{1s}\\\beta_d\end{bmatrix}$$

On the other hand, from equation (24) one can get:

$$\ddot\beta_1\cos(\psi)+\ddot\beta_2\cos\left(\psi+\frac{\pi}{2}\right)+\ddot\beta_3\cos(\psi+\pi)+\ddot\beta_4\cos\left(\psi+\frac{3\pi}{2}\right)=$$

$$(a_{51}\beta_1+a_{55}\dot\beta_1)\cos(\psi)+(a_{62}\beta_2+a_{77}\dot\beta_2)\cos\left(\psi+\frac{\pi}{2}\right)+ \quad (38)$$

$$(a_{73}\beta_3+a_{77}\dot\beta_3)\cos(\psi+\pi)+(a_{84}\beta_4+a_{88}\dot\beta_4)\cos\left(\psi+\frac{3\pi}{2}\right)$$

Comparison of the right sides of the equation (37) and (38) allow determining elements $T_{6,i}$ .As an example, element $T_{6,1}$ is given by:

$$T_{61}=\frac{a_{51}\cos(\psi)+a_{62}\cos\left(\psi+\frac{\pi}{2}\right)+a_{73}\cos(\psi+\pi)+a_{84}\cos\left(\psi+\frac{3\pi}{2}\right)}{2} \quad (39)$$

Equations (40) and (41) are used to calculate other elements of the transformed matrix, which belong to other rows.

(40)
$$\ddot{\beta}_1 \sin(\psi) + \ddot{\beta}_2 \sin\left(\psi + \frac{\pi}{2}\right) + \ddot{\beta}_3 \sin(\psi + \pi) + \ddot{\beta}_4 \sin\left(\psi + \frac{3\pi}{2}\right) =$$
$$[0 \quad 0 \quad 2 \quad 0] \cdot \begin{bmatrix} \ddot{\beta}_0 \\ \ddot{\beta}_{1c} \\ \ddot{\beta}_{1s} \\ \ddot{\beta}_d \end{bmatrix} + [0 \quad -4\Omega \quad 0 \quad 0] \cdot \begin{bmatrix} \dot{\beta}_0 \\ \dot{\beta}_{1c} \\ \dot{\beta}_{1s} \\ \dot{\beta}_d \end{bmatrix} +$$
$$[0 \quad 0 \quad -2\Omega^2 \quad 0] \cdot \begin{bmatrix} \beta_0 \\ \beta_{1c} \\ \beta_{1s} \\ \beta_d \end{bmatrix}$$

(41)
$$-\ddot{\beta}_1 + \ddot{\beta}_2 - \ddot{\beta}_3 + \ddot{\beta}_4 = [0 \quad 0 \quad 0 \quad 4] \cdot \begin{bmatrix} \ddot{\beta}_0 \\ \ddot{\beta}_{1c} \\ \ddot{\beta}_{1s} \\ \ddot{\beta}_d \end{bmatrix}$$

3.3. Example ground resonance

Ground resonance is a self-excited dynamic instability caused by the interaction of the lagging motion of the rotor blades with other modes of the motion of the helicopter and results a violent damage of structure. For a helicopter with soft in-plane rotor, the critical mode is usually an oscillation of the helicopter on the landing gear when it is in contact with the ground. Therefore this instability is called ground resonance.
Some of the most important parameters of this instability are:

- Blade lag frequency
- Blade lag damping
- Frequencies of the structure supporting the rotor

For the classical ground resonance analysis, the degrees of freedom of the helicopters are reduced and just the lag degree of freedom of the rotor blades and longitudinal and lateral in-plane motion of the rotor hub are considered. For this model aerodynamic forces have little influence on the instability effect in compare to structural and inertial forces, therefore aerodynamic forces can be neglected [15]. For a hingeless rotor a more complete model is required, including rotor aerodynamics and flap motion of rotor blades.
The aim of this example is usage of the multiblade coordinates transformation for SIMPACK model. Therefore at this part a simple ground resonance model was selected to avoid any unnecessary complexity. The example "flapping stability of rotor blade in forward flight" which is much more complex, was modelled and analysed using the multiblade coordinate transformation [1].
Fig. 3 shows the ground resonance model created using SIMPACK. For this model the fuselage has two translational degrees of freedom and rotor blades have lagging degree of freedom. Blades were jointed to the lag hinge with rotational springs and dampers. The data related to the rotor are based on the scaled research rotor "BO105, DNW, configuration K20" available in Institute of Aeroelasticity, DLR Göttingen. The SIMPACK rotor model is in fact a mathematically equivalent model of the hingless rotor blade of "BO105". For this mathematically equivalent model the hingless rotor blade is modelled with a rotor with an equivalent lagging hinge and equivalent spring and damping coefficients to model the stiffness and damping of the hingless rotor [16]. Using the "substitution variables" and "ParVariation" options of SIMPACK allows performing parameter studies of the model.

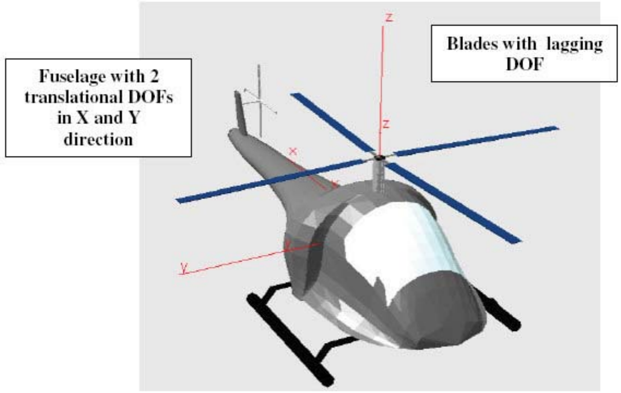

FIG. 3. SIMPACK ground resonance model

In this paper the results of two ground resonance models are introduced.
The data related to the first model are :

Rotor data

0.35 [m]	Distance between the lagging hinge and the axis of rotation.
1.39 [Kg]	Blade mass
1.66 [m]	Blade length
1.281[Kgm²]	Blade mass moment of inertia about lagging hinge
81.6 [Nm/grad]	Lagging stiffness
1.5 [% crit.]	Damping ratio

Fuselage data

160000 [N/m]	Spring stiffness in Y direction
77.519 [Ns/m]	Damping coefficients in Y direction
160700 [N/m]	Spring stiffness in X direction
65 [Ns/m]	Damping coefficients in X direction
3.51 [Hz]	Frequency of eigenform in Y direction for $\Omega = 0$
3.52 [Hz]	Frequency of eifenform in X direction for $\Omega = 0$
0.54 [% crit.]	Damping ratio in Ydirection for $\Omega = 0$
0.45 [% crit.]	Damping ratio in X direction for $\Omega = 0$
322 [Kg]	Fuselage mass

To perform the stability analysis, rotor rotational velocity is changed stepwise. For each value of rotational velocity the system is linearised about the trim state. Then the linear system matrix of the model is extracted and saved in MATLAB m-file format. After that the multiblade coordinate transformation is performed to transform the linear system matrix "$[A]$" from rotating coordinates to non-rotating coordinates. The transformed system matrix is then called matrix "$[T]$". Fig. 4 shows the linear differential equation of the system in rotating and non-rotating coordinates and illustrates the definition of the system matrices. After performing the transformation the eigenvalues of the transformed linear system matrix $[T]$ are determined and with respect to the eigenforms are sorted. The frequencies and damping are then calculated and evaluated.

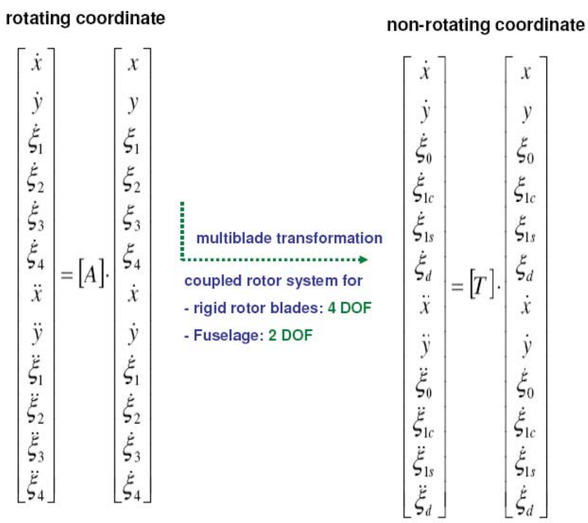

FIG. 4. Multiblade coordinates transformation

A CAMRAD II simulation of the simplified ground resonance model is used to validate the procedures performed for the SIMPACK model. From the data, which are used for SIMPACK model, the data needed for the CAMRAD II model are calculated. This is necessary due to the differences of the structure of the modelling input file of CAMRAD II [17] and SIMPACK. Fig. 5 shows schematically the rotor modelled using CAMRAD II.

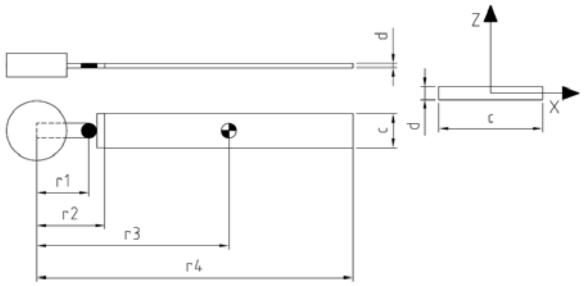

FIG. 5. CAMRADII rotor model

From the mass moment of inertia used for SIMPACK model and the rotor length one can calculate the rotor chord length:

$$b = r4 - r2 = 1.658[m]$$

$$(42)\quad I_{CG} = \frac{m(b^2 + c^2)}{12} = \frac{1.3896(1.658^2 + c^2)}{12} = 0.3245$$

$$\Rightarrow c = 0.2308[m]$$

From the geometry of the rotor blade and its mass the density is calculated.

$$(43)\quad \rho = \frac{M_{blade}}{b \cdot c \cdot d} = \frac{1.3896}{1.658 \cdot c \cdot 0.12c} = 131.1\left[Kg/m^3\right]$$

Equations 44 and 45 give the value of the two other parameters needed in the model input file.

$$(44)\quad I_{THETA} = \int (x^2 + z^2)\rho \cdot dA = 0.00377359[kgm]$$

$$(45)\quad I_{POLAR} = \int (x^2 - z^2)\rho \cdot dA = 0.00366645[Kgm]$$

Fig. 6 shows the frequency and damping of the transformed system matrix of the both SIMPACK and COMRAD II models. Comparison of the results of both simulation tools shows the agreement of them and validates the implemented MATLAB program for multiblade transformation.
According to the Fig. 6 the ground resonance of the model happens by rotational frequency ~17 [Hz]. This instability happens when the regressing frequency of the rotor interfaces the fuselage frequency. However this happens in two different points. Investigating the damping on the interfaces shows that just in one interface the damping of the fuselage eigenform reduces and leads to instability. The instability of this ground resonance model depends to the following parameters:
natural frequencies of the helicopter and the blades, the distance between the rotor hub and the lead-lag hinge, the moment of inertia of a blade about the lead-lag hinge, the rotor speed, the mass of blade, and the effective mass of the hub. To see the effect of each of these parameters on the stability, one can perform parameter studies using the parameter variation option of SIMACK “ParVariation”.

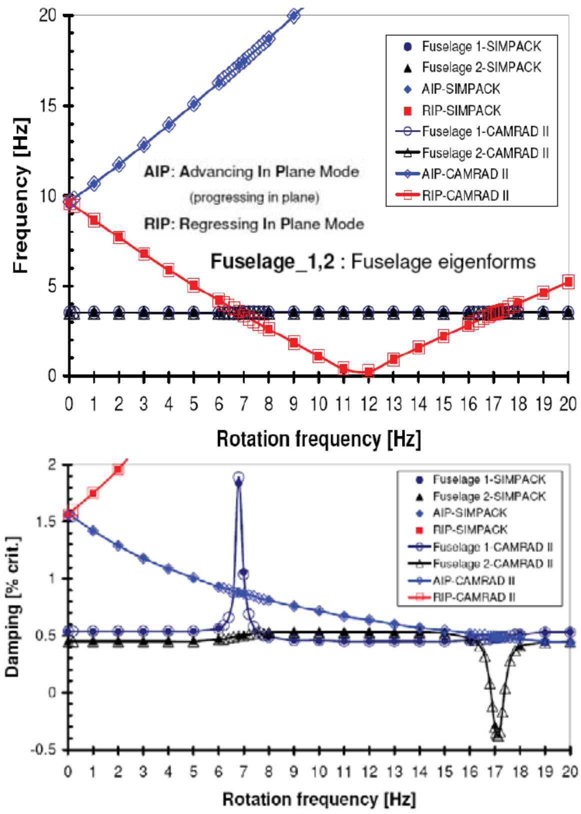

FIG. 6. Frequency and damping of the eigenvalues of the transformed system matrix, first model

By the first ground resonance model the frequencies of the eigenforms of the fuselage in both X and Y direction have nearly the same values. For the next model these frequencies have different values and they are far from each other. The data used for this model are:

Rotor data

Same data used for the first model

Fuselage data

31135 [N/m] Spring stiffness in Y direction
143 [Ns/m] Damping coefficients in Y direction
15645000 [N/m] Spring stiffness in X direction
6500 [Ns/m] Damping coefficients in X direction
3.48 [Hz] Frequency of eigenform in Y direction for $\Omega = 0$
79.17 [Hz] Frequency of eigenform in X direction for $\Omega = 0$
5 [% crit.] Damping ratio in Y direction for $\Omega = 0$
10.39 [% crit.] Damping ratio in X direction for $\Omega = 0$
59.09 [Kg] Fuselage mass

These data were used for both SIMPACK and CAMRADII models. Fig. 7 shows the final results of the both simulation tools. Comparison of the results shows the agreement of them and again validates the procedures used for SIMPACK model.

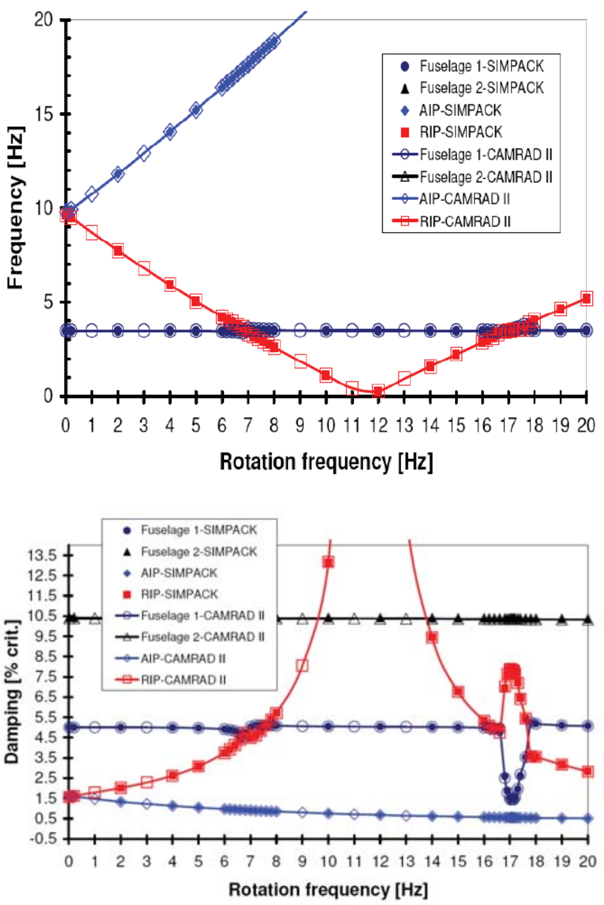

FIG. 7. Frequency and damping of the eigenvalues of the transformed system matrix, second model

Analysing the damping curves shows that at the point of instability the energy needed for increasing of the amplitude of the fuselage oscillation comes from the rotor (increasing of the rotor damping equals to reducing the energy).

4. CONCLUSION

Existing modelling options and features of SIMPACK which are used to analyse rotating systems were evaluated. Among all the options, the following were evaluated by performing the different simulations [1]:

- Rotational effects
- Linearization of the nonlinear system
- Parametric modelling and studies
- Expressions (user defined functions)
- Post-processing

For evaluation of the simulation results, the SIMPACK results were compared with analytical solutions and in some other cases with the results of other simulation tools. The evaluation of the results leads to the following statements:

- For a rotating system, SIMPACK considers the forces resulting from rotation.
- Linearization option of SIMPACK gives valid results. This statement should be tested for more complex systems.
- SIMPACK allows defining parameters inside the model and performing different analysis with parameter variation. For example eigenvalue analysis of a rotor can be performed for different rotational velocity, by defining this as model parameter.
- SIMPACK allows creating functions inside the model and let them be used for different parameters of the model. This option enables us to create the multiblade coordinates as functions and request them as outputs.
- In most cases SIMPACK can be used as postprocessor for evaluation of the results. Features of SIMPACK like frequency analysis "FFT, fast Fourier transformation" or creating filters are its advantages.

Two mathematical methods for multiblade transformation were stablished. These two methods were formulated and later implemented using MATLAB. The results of both methods were compared. This allowed checking the methods. Both methods produce the same result for the same input.
Different examples of ground resonance were modelled using CAMRAD II and SIMPACK and the results of simulation were compared together. Comparisons show the validity of the Modelling and analysis procedures using SIMPACK.
For usage of the Floquet theory, some models were simulated using SIMPACK. The comparison of the results of stability analysis using Floquet theory and the behaviour of the system during the time integration of the system shows the validity of the methods used. This has been checked for different models and examples [1].
The limitation of the method introduced, for performing the stability analysis using Floquet theory, for a system with high numbers of state variables should not be neglected. Usage of methods like "implicit Floquet theory" should overcome this limitation.

5. ACKNOWLEDGMENT

This paper is the result of a diploma thesis at RWTH Aachen. The subject of this thesis was defined by Eurocopter Germany.
I would like to express my gratitude to my supervisor Mr. Oliver Dieterich, Eurocopter Germany, for his scientific and technical support and discussion and his helpful comments in writing the diploma thesis.
I would also like to thank Dr. G. Neuwerth and Prof. R. Henke, ILR RWTH Aachen, for their support and supervision of my diploma thesis.
Next, I would like to sincerely thank Dr. F. Kiessling, Dr. W. Krüger, Institute of Aeroelasticity DLR Göttingen, for all their technical and scientific support, all their helpful comments and suggestions.

6. REFERENCES

[1] A. Rezaeian, Stability Analysis of Time-periodic Systems Using Multibody Simulation for Application to Helicopters, Diploma thesis, Institute of aeronautics and astronautics, RWTH Aachen, March 2009.
[2] W. Kliemann, N. Sri Namachchivaya, Nonlinear Dynamics and Stochastic Mechanics, by CRC Press, Inc., ISBN 0-8493-8333-1, 1995
[3] L.Prandtl, Beitrage zur Frage der kritischen Drehzahlen. Dinglers Polytechnisches Journal (20)330, 179-182 (1918).
[4] W. Cambell, Protection of steam turbine disk wheels from axial vibration. Trans. ASME 46, 31-160 (1924).
[5] Olivier A. Bauchau, Yuri G. Nikishkov , An Implicit Floquet Analysis for Rotorcraft Stability Evaluation, journal of the American Helicopter Society, July 2001. Volume 46- Number 3.
[6] Lowis, O.J., The Stability of Rotor Blade Flapping Motion at high Tip Speed Ratios, Reports and Memoranda No. 3544, Aeronautical Research Council, University of Southhampton, January 1963.
[7] David A. Peters, Fast Floquet Theory and Trim for Multibladed Rotorcraft, Journal of the American Helicopter Society, Volume 39- Number 4, October 1994.
[8] David A. Peters, Kurt H. Hohenemser, Application of the Floquet Transition Matrix to Problems of Lifting Rotor Stability , Journal of the American Helicopter Society, Vol.16,No.2, April 1971, pp.25-33.
[9] C. Von Kerczek, S.H. Davis, Calculation of Transition Matrices, AIAA Journal,vol.13,No.10, October 1975, pp. 1400-1403.
[10] P. Friedmann, C.E. Hammond, T.H. Woo, Efficient Numerical Treatment of Periodic Systems with Application to Stability Problems, International Journal for Numerical Methods in Engineering, Vol.11, 1977, pp. 1117-1136.
[11] Robert P. Coleman, Arnold M. Feingold, Theory of Self-Excited Mechanical Oscillations of Helicopter Rotors with Hinged Blades, NACA Technical Report TR 1351, 1958.
[12] Wayne Johnson, Helicopter Theory, Dover publication, Inc., New York, ISBN 0-486-68230-7, 1994.
[13] SIMPACK, SIMPACK Reference Guide, SIMPACK release 8.8, 16th March 2006, SIMDOC v8.800, Copyright INTEC GmbH2006.
[14] Michael A. Gockel, Practical Solution of Linear Equation with Periodic Coefficients, Staff, Rotary Wing Technology Division, Lockheed-California Co., Burbank, California, Journal of the American Helicopter Society, January 1972.
[15] Richard L. Bielawa, Rotary Wing Structural Dynamics and Aeroelasticity, AIAA, Inc., Washington, DC, ISBN 1-56347-031-4, 1992
[16] H.-J. Langer, F. Kiessling, Dr. R. Schröder, A Model for Windtunnel Rotorcraft Research, Ground Resonance Investigation, Second European Rotorcraft and Powered Lift Aircraft Forum, Paper No. 33, 1976.
[17] CAMRAD II, Comprehensive Analytical Models of Rotorcraft Aerodynamics and Dynamics, Volume VI, Rotorcraft Input, Release 4.6, Wayne Johnson, Johnson Aeronautics, Palo Alto, California, 2007.